Scientific Research Publishing

Open Journal of Inorganic Chemistry, 2025, 15(1), 1-22
https://www.scirp.org/journal/ojic
ISSN Online: 2161-7414
ISSN Print: 2161-7406

Synthesis, Characterization, Spectral Analyses, Antimicrobial Activities, and Computational Studies of Some Transition Metal Complexes of N'-(2-oxo-2H-chromen-4-yl) Nicotinohydrazide

Romanus N. Njong[1*], Ankoro Naphthali[2], Gwendoline M. Toh-Boyo[2], Cyprian C. Mikwa[2], Emmanuel N. Nfor[2]

[1]Department of Fundamental Science, Higher Technical Teachers Training College, The University of Bamenda, Bamenda, Cameroon
[2]Department of Chemistry, Faculty of Science, University of Buea, Buea, Cameroon
Email: *njong74@gmail.com, njong.romanus@uniba.cm, nfor.emmanuel@ubuea.cm

How to cite this paper: Njong, R.N., Naphthali, A., Toh-Boyo, G.M., Mikwa, C.C. and Nfor, E.N. (2025) Synthesis, Characterization, Spectral Analyses, Antimicrobial Activities, and Computational Studies of Some Transition Metal Complexes of N'-(2-oxo-2H-chromen-4-yl) Nicotinohydrazide. *Open Journal of Inorganic Chemistry*, **15**, 1-22.
https://doi.org/10.4236/ojic.2025.151001

Received: December 23, 2024
Accepted: January 28, 2025
Published: January 31, 2025

Abstract

The metal complexes Cu (II), Zn (II), and Co (III) complexes of (N'-(2-oxo-2H-chromen-4-yl) nicotinohydrazide, a derivative of *nicotinic acid hydrazide condensed with* 4-*hydroxycoumarin,* have been synthesized. The ligand and its metal complexes were characterized by various physico-chemical and spectroscopic tools, viz: Elemental Analysis, FT-IR, TGA, ^{1}H NMR, UV-visible, molar conductance, and magnetic susceptibility as well as theoretical computation. On the basis of these analyses, the ligand was found to coordinate to metal ions in a tridentate mode through the nitrogen atom of the azomethine group and the oxygen atom of the ketonic groups. The spectral and magnetic data allowed for the chemical structures of the metal complexes to be predicted, wherein octahedral geometry was assigned to the Co (III) complexes, while tetrahedral geometry was assigned to the Cu (II) and Zn (II) complexes; this was further explored in a DFT calculation. Conductance measurement suggested the non-electrolytic nature of the compounds. The anti-tubercular activities of the compounds showed zinc (II) and copper (II) complexes having identical activity to the reference drugs, pyrazinamide and isoniazid, while the cobalt (III) complex had the highest MIC value compared to the reference drugs and parent ligand.

Keywords

Complexes, Hydrazones, Computational, Anti-Tubercular Activity, Nicotinic Acid Hydrazide

1. Introduction

Hydrazones, as Schiff bases derived from the condensation reactions of hydrazine as primary amines with carbonyls, have gained increasing interest in research due to their physiological properties and coordination abilities to stabilize metal ions of different oxidation states. Experiments to demonstrate the effect of metal ions on metal-ligand stoichiometry and a broad spectrum of biological activities of their complexes have been increasing steadily for many years [1]-[7]. Aroylhydrazones have an additional C=O function and thus are characterized by the presence of Ph-CO-NH-N=C< donor sites, which can act in monodentate, bidentate, or tridentate coordination mode to metal ions, providing the versatility and flexibility of these compounds; thus, aroylhydrazones are famous ligands [8]-[11]. Hydrazones containing –N-NH-CO– groups have been at the forefront in the development of symmetrical dihydrazone transition metal complexes, as they demonstrate versatility in their coordination mode and a tendency to show stoichiometry due to their high coordination numbers [12]-[14].

Isoniazid, otherwise called Isonicotinoylhydrazide (INH), introduced in 1952 as an Anti-Tuberculosis (TB) agent, is generally administered in combination with rifampin, pyrazinamide, streptomycin and/or ethambutol in the first-line treatment of TB [15]. Isoniazid derivatives containing a heterocyclic moiety have been found to exhibit greater anti-microbial activities than isoniazid itself [16]-[19]. Also, coumarins (benzopyran-2-one or chromene-2-one) are an important class of bioactive oxaheterocyclic ring systems of the lactone family, which have been found to reveal interesting antimicrobial, antifungal, anti-inflammatory, anti-cancer, anti-tubercular, antioxidant, and anticoagulant properties [20]. The substitution patterns of phenolic groups present at the coumarin nucleus of various derivatives as well as biological activity are related, and 4-hydroxycoumarin is an important precursor in organic synthesis; its derivatives have shown a remarkably broad spectrum of biological activities [21] [22]. Schiff bases derived from coumarin and its metal complexes have been found to exhibit antibacterial, antifungal, anticoagulation, and plant-regulating activities [23]-[25].

In view of the above considerations and in continuation of our investigations of metal complexes derived from hydrazide-hydrazone ligands, we hereby report on some transition metal (II)/metal (III) complexes derived from a novel Schiff base containing both Isonicotinoylhydrazide and 4-hydroxycoumarin moieties bonded through the azomethine linkage.

2. Materials and Methods

All chemicals and solvents used for syntheses were of analytical grade and used without further purification except the solvents. Elemental analysis was performed on a Thermo Flash EA-1112 Series CHNS-O Elemental Analyzer. The IR spectra were obtained from KBr pellets in the range 4000 - 400 cm^{-1}, using a Perkin-Elmer Spectrum 100 FT-IR spectrometer. ^{1}H NMR spectra were recorded on a Varian Unity plus 400 MHz instrument. TGA measurements were performed at a heating

rate of 10˚C/min in the temperature range 25 - 600˚C, under dry nitrogen flow rate of 60 mL/min on a TGA Q500 instrument. Approximately 2 - 5 mg of sample was placed in an open aluminum crucible.

2.1. Synthesis of Ligand: N'-(2-oxo-2H-chromen-4-yl) Nicotinohydrazide

4-hydroxycoumarin (1.500 g, 0.01 mol) dissolved in 15 mL ethanol was added to nicotinic acid hydrazide (1.269 g, 0.01 mol) in 10 mL of ethanolic solution and 3 drops of glacial acetic acid as a catalyst. The resulting mixture was refluxed for 5 hours at 80˚C while stirring. The yellow product obtained was left overnight to cool, removed by vacuum filtration, washed several times with water, ethanol, and diethyl ether, and left to recrystallize from ethanol. TLC on pre-coated silica-gel plates was used to check the purity of the compound (Scheme 1). Attempts to grow crystals of LH after 30 days for single crystal X-ray diffraction studies proved unsuccessful (**Figure 1**).

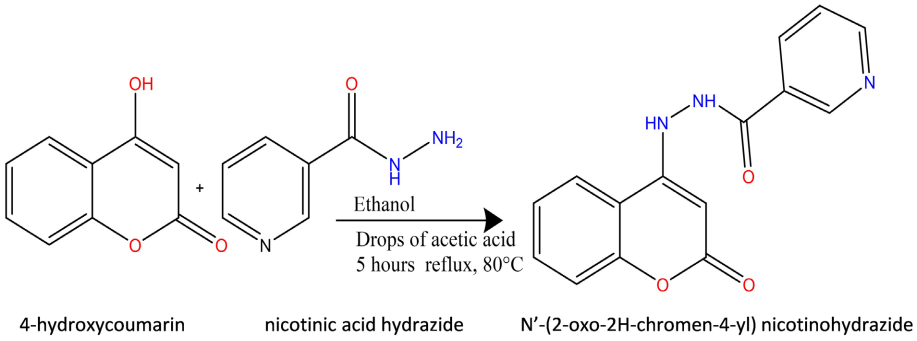

Figure 1. Synthesis of N'-(2-oxo-2H-chromen-4-yl) nicotinohydrazide.

2.2. Synthesis of Metal Complexes

The metal complexes Cu (II), Zn (II), and Co (III) were prepared by the addition of ethanolic solution of Copper (II) acetate monohydrate (0.199 g, 1.0 mmol), Zinc (II) chloride (0.136 g, 1.0 mmol), or Cobalt (III) acetate (0.236 g, 1.0 mmol), respectively, to the ligand N'-(2-oxo-2H-chromen-4-yl) nicotinohydrazide (0.563 g, 2.0 mmol) in 25 mL ethanolic solution. The resulting mixture was refluxed for 5 hours at 90˚C while stirring continuously using a magnetic stirrer. The resulting colored products obtained were allowed to cool overnight, the precipitate was removed by filtration, washed with ethanol, and exposed to air drying. The filtrate obtained was allowed for crystal growth, with no crystal formed after 60 days. The compounds obtained were all solids and were then characterized by various physico-chemical methods.

2.3. Anti-Tuberculosis Evaluation

The antimicrobial activities of the novel hydrazone ligand (LH), its metal (II) and metal (III) complexes, were evaluated against *M. tuberculosis* (ATTC 27294) using

the Alamar Blue susceptibility test, and the activity was expressed as the Minimum Inhibitory Concentration (MIC) in μg/mL according to the method reported by Maria and Lourenco [22] [26]. The Minimum Inhibitory Concentration (MIC) was determined for each derivative, measured as the minimum concentration of the compounds required to completely inhibit bacterial growth. The reference drugs used to evaluate the potency of the synthesized compounds were streptomycin (MIC = 6.25 ± 0.72 μg/mL) ± SD, pyrazinamide (MIC = 3.12 ± 0.34 μg/mL) ± SD, and isoniazid (MIC = 3.12 ± 0.34 μg/mL) ± SD.

2.4. Computational Studies

Molecular modeling was done with the Orca program in the gas phase using density functional theory. Prior to the DFT calculation, the ligand and its metal complexes were pre-optimized through conformer search using molecular mechanics methods in Avogadro 1.2.1 software [27].

3. Results and Discussion

3.1. The Physical Properties of the Ligand and Its Metal Complexes

The physical properties of the ligand and its metal complexes are shown in **Table 1**. The colours of the ligand and its metal complexes range from ash to reddish brown, different from those of the metal salts and the ligand (white) used, which is an indication that the compounds obtained were new. Colour variation and formation of precipitate were the physical parameters used to track the progress of the synthetic reaction. The ligands and their corresponding metal complexes were all powdery solids at room temperature. The melting points of the compounds range from 178˚C to 290˚C, which are different from those of the ligand precursors and the metal salts used. The melting points of both the ligands and the metal complexes were all sharp, an indication that these compounds were very pure. All the prepared compounds were very soluble in DMSO but slightly soluble in methanol and methylene chloride, and insoluble in hexane and ethyl acetate.

Table 1. Physical properties of the ligand LH and its metal complexes.

Compound	Melting Point/˚C	Physical State	Colour	% Yield
$C_{15}H_{11}N_3O_3$(LH)	178	solid	White	70
$[Zn(C_{15}H_{11}N_3O_3)_2]$	225	solid	White	75
$[Cu(C_{15}H_{11}N_3O_3)_2]$	248	solid	Reddish-brown	82
$[Co(C_{15}H_{11}N_3O_3)_2(Ac)_2]^+$	260	solid	Brown	80

3.2. Spectral Analysis of the Ligand and Its Metal (II) Complexes

3.2.1. Infrared Spectra

The infrared spectra of the free ligand LH and its metal (II)/metal (III) complexes (**Figures 2-5**) revealed characteristic broad absorption bands in the

region 3425 - 3650 cm^{-1} and 3000 - 3015 cm^{-1}, corresponding to νO-H and νN-H stretching vibrations, respectively [26]. In the spectrum of the hydrazone ligand, strong bands observed at 1750 and 1550 cm^{-1} were attributed to ν (C=O) and ν (C=N), respectively [28]. In the spectra of the metal(II)/metal(III) complexes, the ν (C=O) and ν (C=N) bands of the free ligand shifted to lower frequencies of 1625 and 1500 cm^{-1} in the cobalt (III) complex; 1650 cm^{-1} and 1510 cm^{-1} in the copper (II) complex; and 1630 cm^{-1} and 1525 cm^{-1} in the zinc(II) complex, respectively, indicating coordination through the amide oxygen and the azomethine nitrogen atoms [29]. Moreover, the metal complexes displayed the ν (M-N) and ν (M-O) bands in the region 550 - 580 cm^{-1} and 450 - 470 cm^{-1}, confirming the coordination of the amide oxygen and the azomethine nitrogen to the metal ions [30] [31]. Bands appearing at 995, 939, 800, and 781 cm^{-1} in the spectrum of LH ligand are the usual modes of aromatic ring vibrations and these reveal small shifts in the complexes compared to the free ligand, which is due to the expected electronic structure changes upon coordination. Bands appearing at 995, 939, 800, and 781 cm^{-1} in the spectrum of LH are the usual modes of aromatic ring vibrations and these reveal small shifts in the metal(II) complexes compared to the free ligand, which is due to the expected electronic structure changes that occur with coordination of the ligand to metal ions [17] [18].

3.2.2. Proton NMR

In order to further elucidate the structural features of the ligand synthesized (Scheme 1) and its metal (II)/metal (III) complexes, the ^{1}H NMR spectra of the prepared compounds shown in **Figures 6-9** were obtained in DMSO-d_6 solution. In the ^{1}H NMR spectrum of the ligand, the signal at δ (11.30) (s, 1H) is assigned to the hydroxy proton (–OH) group on the 4-hydroxycoumarin moiety or otherwise formed from amide CO reduction; the signal at δ (9.05) was assigned to the azomethine proton, the doublet in the range δ (8.27 - 8.24) (2H, 2NH) is assigned to the dihydrazone protons, while the signals at δ (7.26 - 6.96) (m, 8H) are due to the aromatic protons of the pyridinyl and coumarin ring moieties, respectively. In the spectra of the metal complexes, these values generally experienced a downfield shift to δ (10.81 - 10.84) (s, 1H) and δ (11.97) (s, 1H) for the hydroxy proton (–OH), δ (9.11, 8.26) (d, 2NH) for the dihydrazone proton (2N-H), respectively. This supports the fact that the coordination of the ligand to the central metals is through the azomethine N and the carbonyl oxygen of the nicotinic acid hydrazide moiety [19] [28]. In the spectra of Cu (II), Zn (II), and Co (III) complexes, signals between δ (9.11 - 8.82), δ (8.29), δ (9.08 - 8.80), and δ (10.81 - 8.28) were assigned to the dihydrazone protons, respectively (**Figure 10** and **Figure 11** and **Table 2**). This supports the fact that the coordination of the ligand to the central metal in each could be through the azomethine N and the carbonyl oxygen of the nicotinic acid and hydrazide moieties [19] [28].

Table 2. IR and ^{1}H-NMR spectroscopic data of ligand LH and its complexes.

Compounds	υO-H	υN-H	υC=O	υC=N	υN-N	υM-N	υM-O	Chemical shifts (δppm)
$C_{15}H_{11}N_3O_3$(LH)	3560	3010	1750	1550	1250	-	-	11.38(1H, s, OH), 9.05 - 8.24 (3H, 3s, HC=N, 2NH), 7.64 - 6.96(8H, Ar-Hs).
$[Co(C_{15}H_{11}N_3O_3)_2]$	3560	3012	1625	1500	1380	625	475	11.95 (1H, s), 9.11, 8.26 (2NH, d), 10.81 - 10.83 (1H, s).
$[Cu(C_{15}H_{11}N_3O_3)_2]$	3560	3015	1650	1510	1275	575	460	10.81 (1H, s), 8.26 (C=NH, s).
$[Zn(C_{15}H_{11}N_3O_3)_2]$	3425	3015	1630	1525	1200	620	450	8.79 (1H, s), 7.61 (C=NH, s).

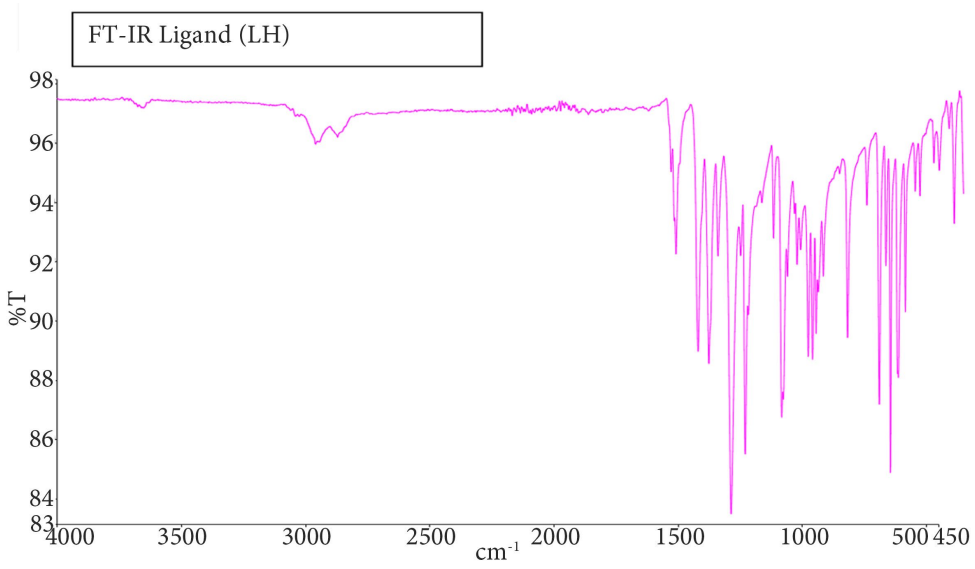

Figure 2. IR spectrum of ligand (LH).

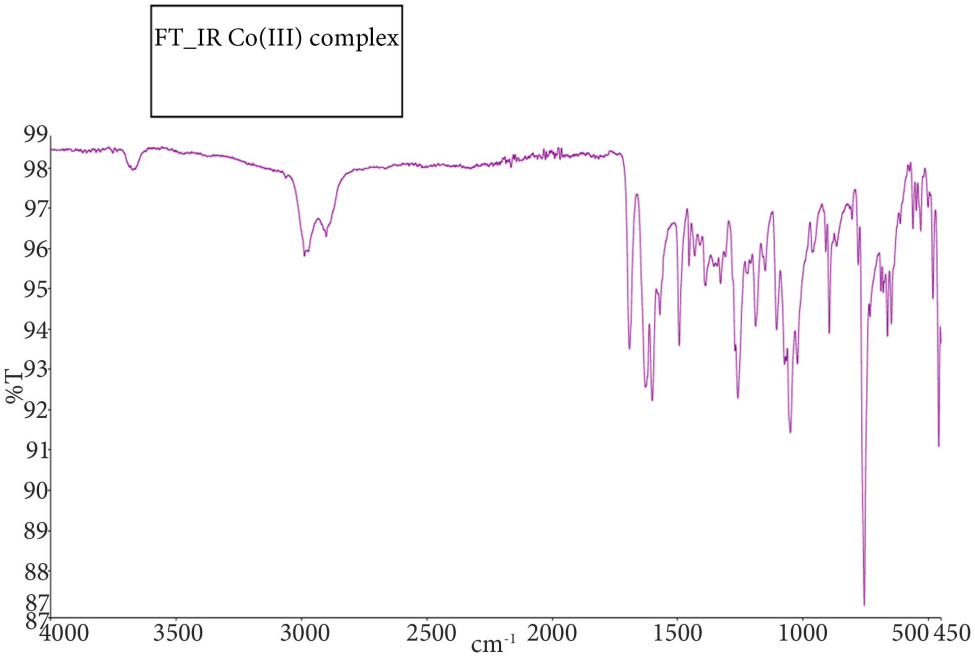

Figure 3. IR spectrum of Co (III) complex.

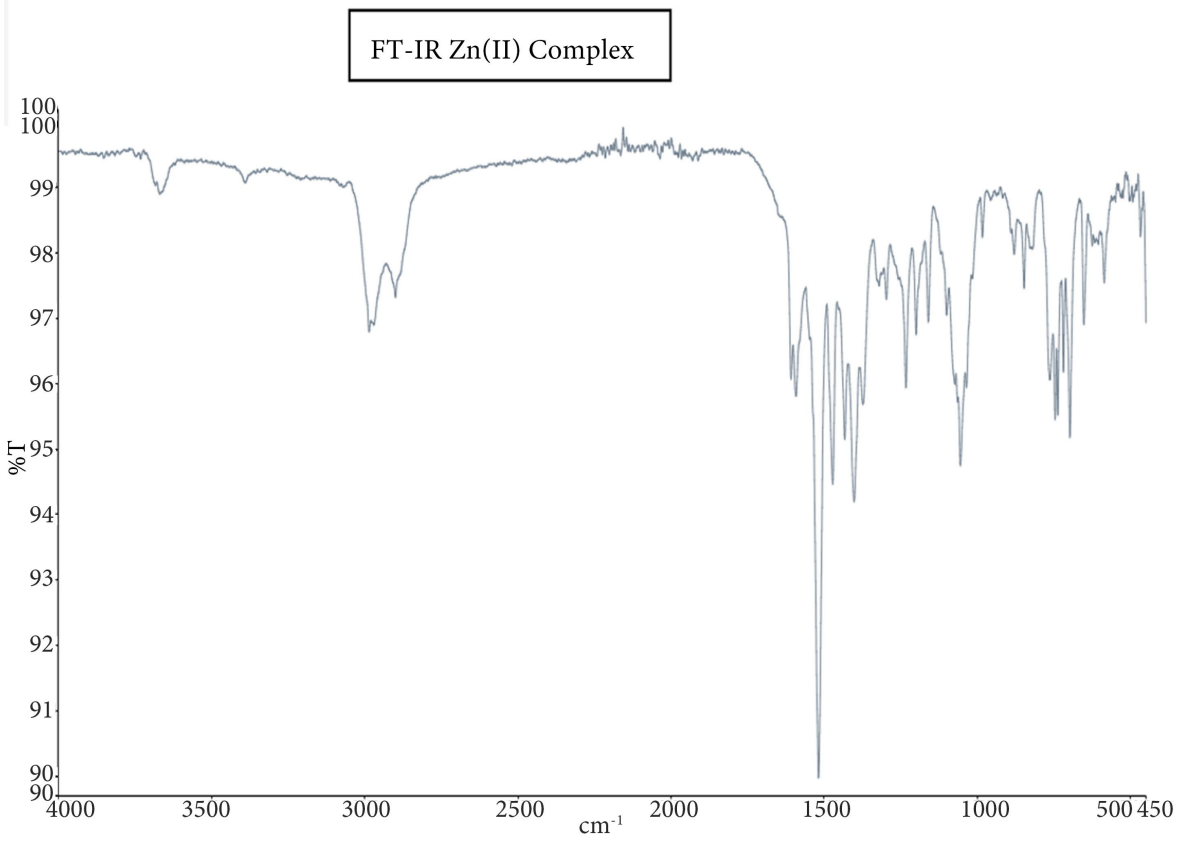

Figure 4. Spectrum of the Zn (II) complex.

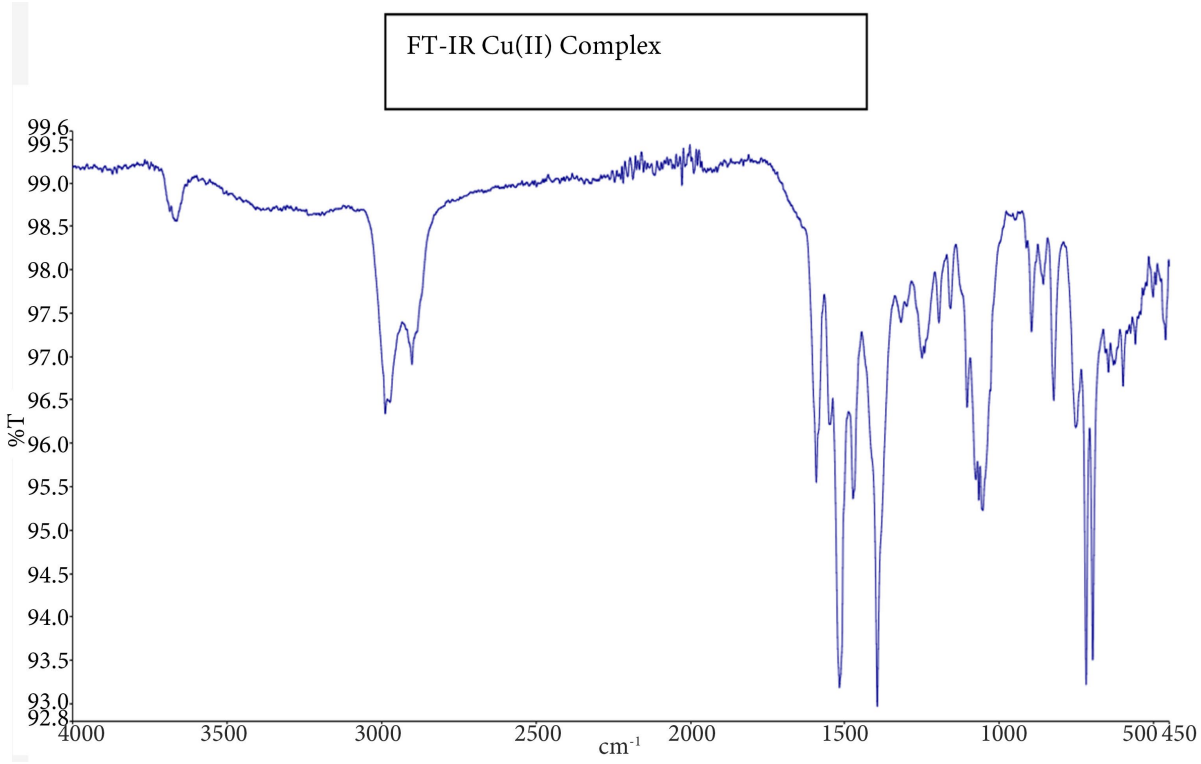

Figure 5. IR spectrum of Cu (II) complex.

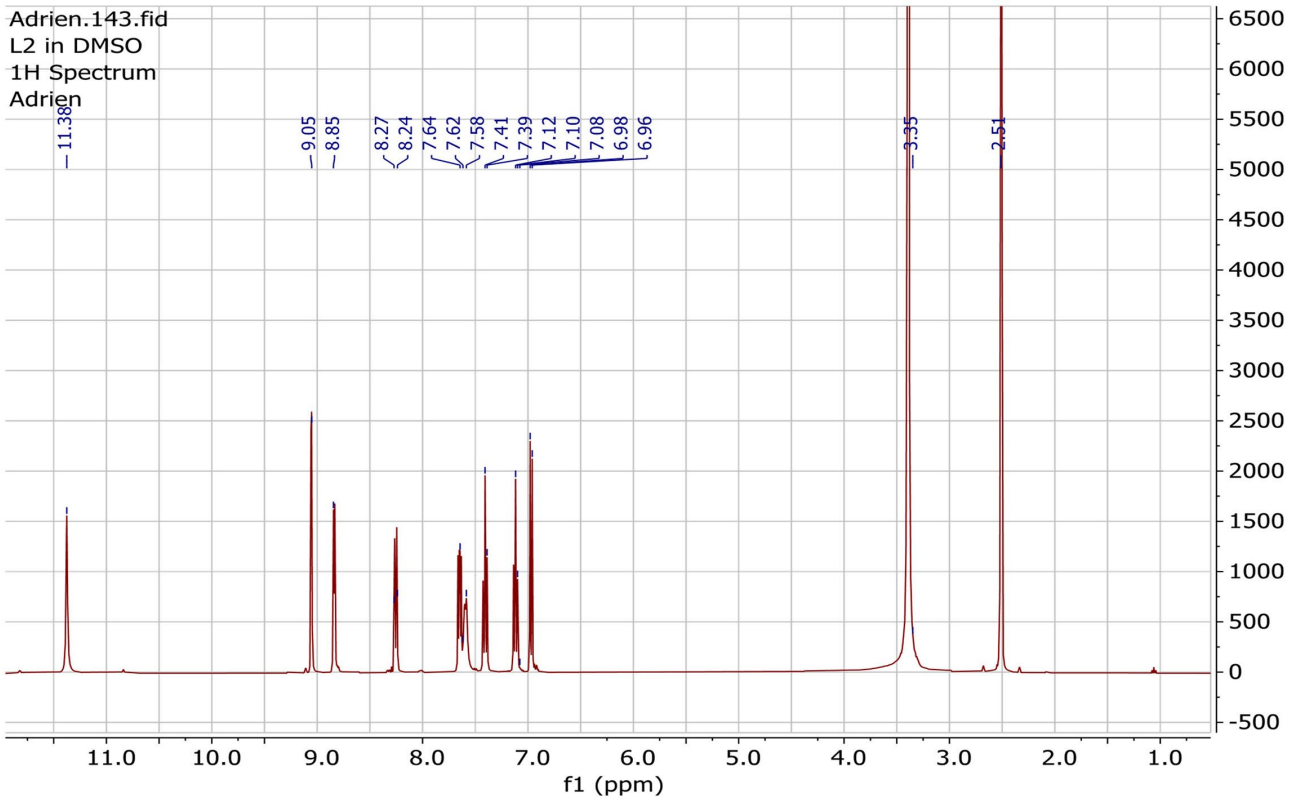

Figure 6. H-NMR spectrum of Ligand (LH).

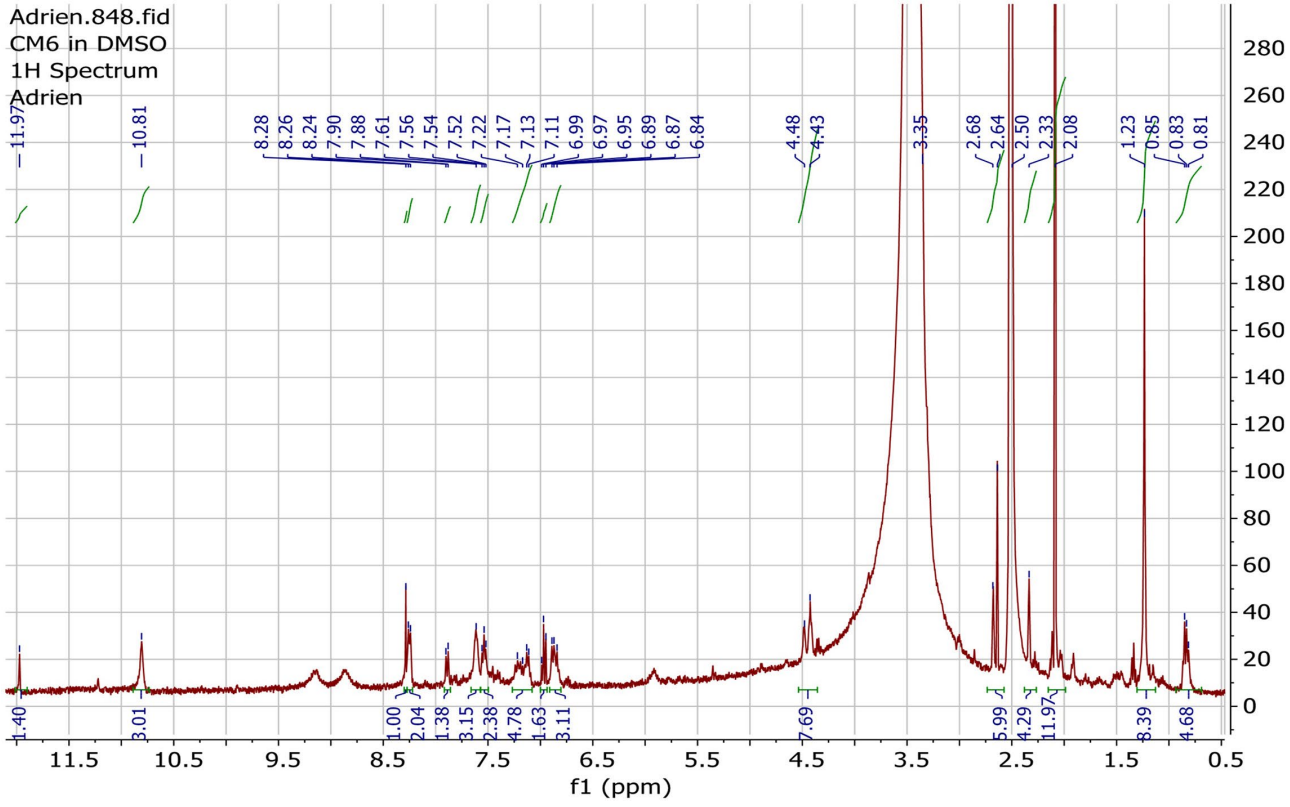

Figure 7. H-NMR spectrum of the Co (III) complex.

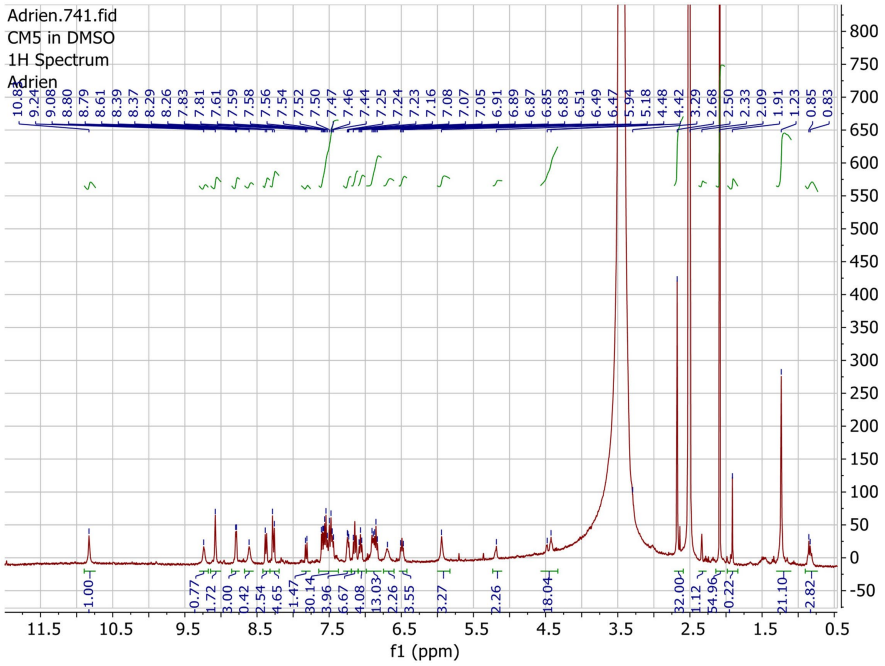

Figure 8. H-NMR spectrum of Zn (II) complex.

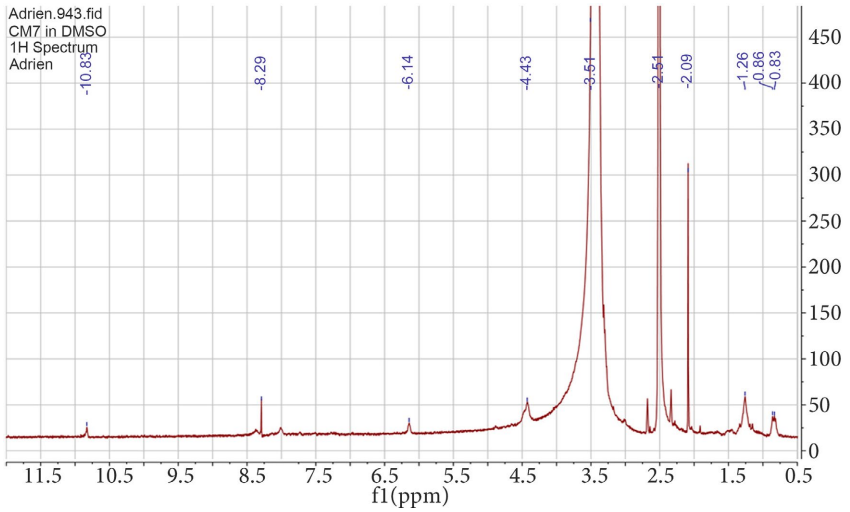

Figure 9. H-NMR spectrum of Cu (II) complex.

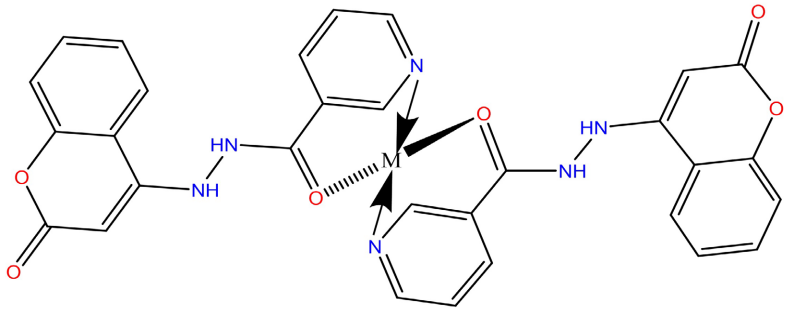

M = Cu(II), Zn (II).

Figure 10. Proposed structures of the tetrahedral complexes.

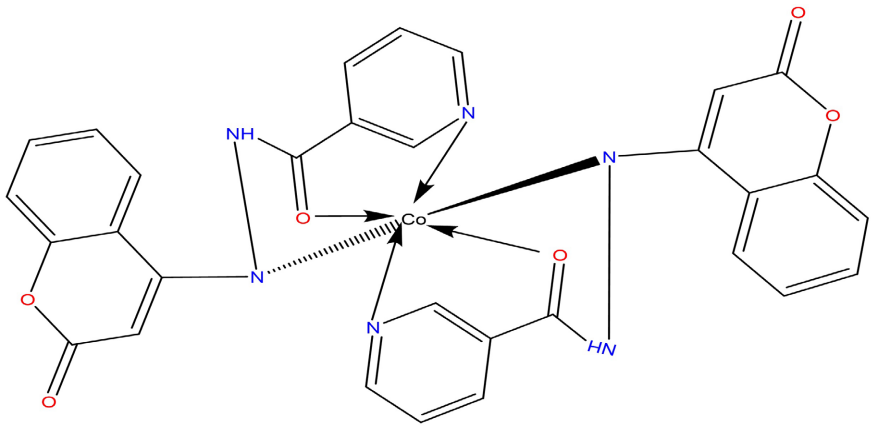

Figure 11. Proposed structure of the octahedral Co (III) complex.

3.2.3. Thermal Analysis of the Ligand (LH) Metal Complexes

The thermogravimetric data of the complexes were recorded within the temperature range of 20˚C to 620˚C and at a heating rate of 20˚C/min in the nitrogen atmosphere as shown in **Figures 12-14**. For the metal complexes, their thermogravimetric analyses were in good agreement with the percentage composition data [30]. The thermogram of zinc (II) complex (**Figure 12**) showed three-step decomposition in the temperature range of 24˚C - 520˚C. In the first step, it showed a mass loss of 4.36% (4.98%, Calc'd) between the temperature 24˚C to 146˚C due to the desorption of the first guest water molecules from the complex. In the second step, between the temperature range of 146˚C to 420˚C, a mass loss of 21.89% (21.35%, Calc'd) was observed due to the desorption of coordinated acetate ions and a nicotinic acid hydrazide acid moiety from the complex. In the third step, a mass loss of 30.82% (30.86%, Calc'd) due to the decomposition of a ligand and 4-hydroxycoumarin moiety was observed within the temperature range of 420˚C to 520˚C, leading to the formation of ZnO [30] [31].

The thermogram of the cobalt (III) complex is shown in **Figure 13**, in which a two-step decomposition process within the temperature range of 20˚C - 540˚C was observed. In the first step, in the temperature range 20˚C to 124˚C, the percentage mass loss of 11.98% (10.44%, Calc'd) is attributed to the desorption of guest molecules (water and uncoordinated acetate ion). The complex was stable up to the temperature of 170˚C, and in the second step, within a temperature range of 170˚C to 540˚C, a mass loss of 61.34% (61.14%, Calc'd) is due to the decomposition of the complex leading to the formation of Co_2O_3 [32] [33].

The thermogram of the copper (II) complex (**Figure 14**) showed a two-step decomposition process within the temperature range of 22˚C - 542˚C. In the first step, within the temperature range of 22˚C to 120˚C, a percentage mass loss of 5.17% (7.93%, Calc'd) is attributed to the desorption of the guest molecule (uncoordinated acetate ion). The second-step decomposition process was observed within the temperature range of 195˚C to 542˚C, amounting to a percentage mass loss of 55.35% (55.96%, Calc'd), due to the decomposition of the complex and finally leading to the formation of CuO [32] [33].

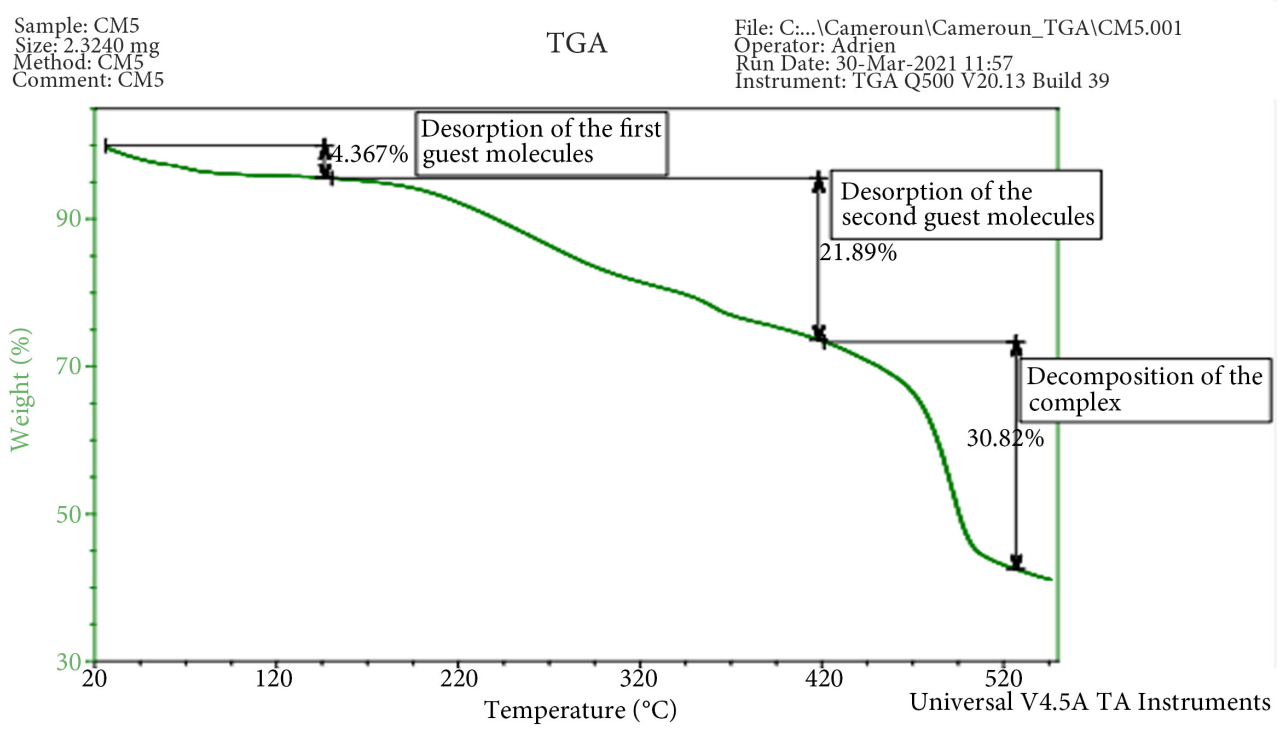

Figure 12. TGA thermogram of the zinc (II) complex of LH.

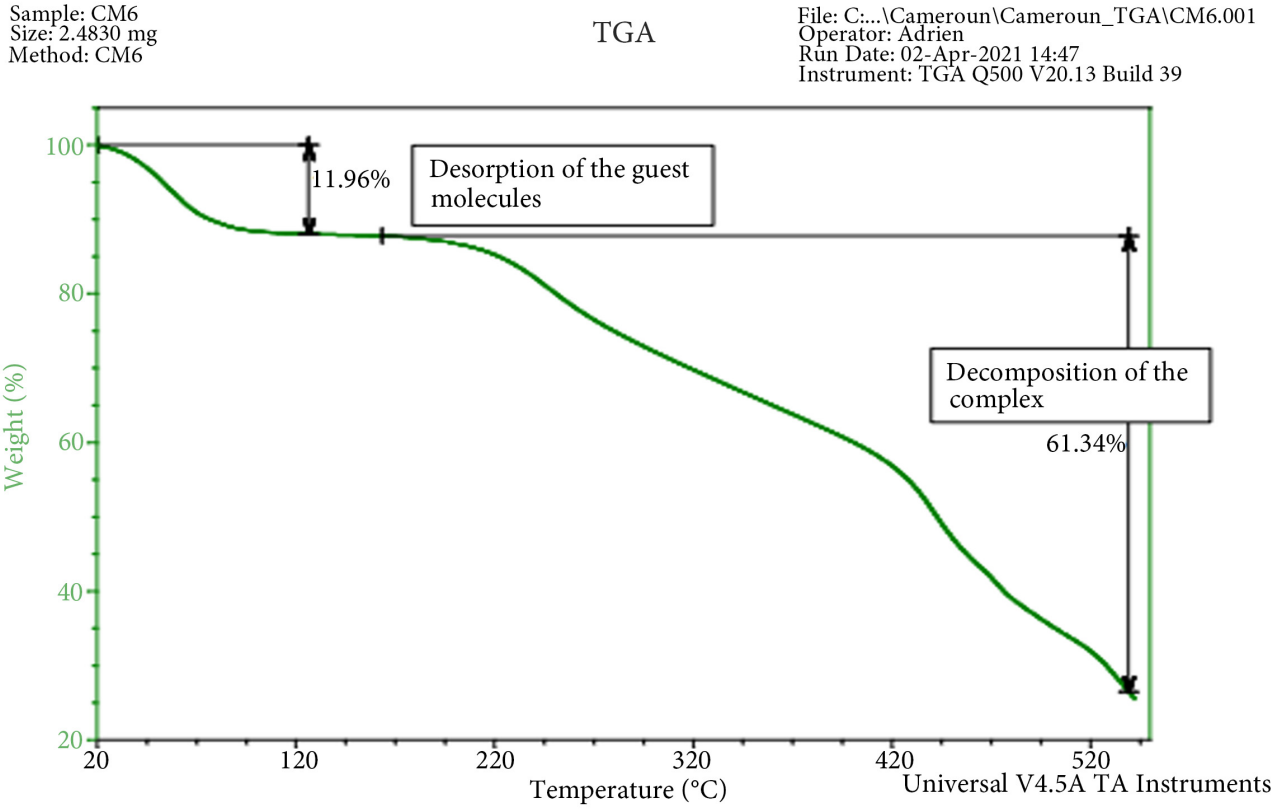

Figure 13. TGA thermogram of the cobalt (III) complex of LH.

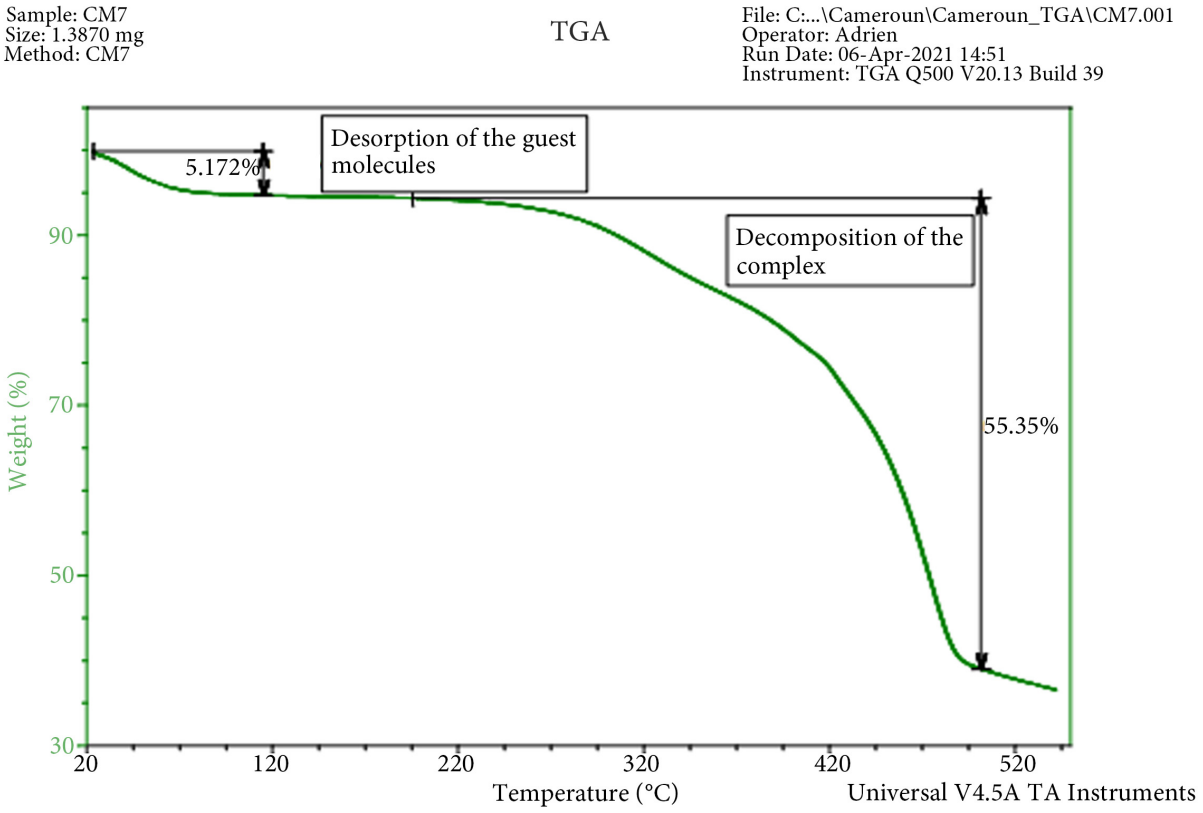

Figure 14. TGA thermogram of the copper (II) complex of LH.

3.2.4. Electronic Spectra

The electronic spectra of the ligand and its metal complexes were recorded between 200 - 800 nm at 298 K in DMSO solvent, in which they were soluble and their absorption bands could easily be seen (**Figure 15** and **Table 3**).

Table 3. Electronic spectral data of the ligand and its metal complexes.

Empirical formula		$[C_{15}H_{11}N_3O_3(LH)]$	$[Zn(C_{15}H_{11}N_3O_3)_2]$	$[Cu(C_{15}H_{11}N_3O_3)_2]$	$[Co(C_{15}H_{11}N_3O_{3)2}\ (Ac)_2]^+$
Molar mass/(amu)		281.27	627.93	626.09	739.56
Elemental Analysis, Found (Calc.) %	C	64.05 (63.96)	54.67 (51.56)	54.83 (54.83)	55.22 (55.17)
	H	3.94 (3.91)	3.15 (3.17)	3.22 (3.77)	3.82 (3.79)
	N	14.94 (14.93)	12.02 (12.03)	11.29 (11.29)	11.36 (11.36)
	O	17.06 (117.06)	13.74 (13.74)	21.50 (21.50)	21.63 (21.63)
	M		9.36 (9.36)	8.54 (8.54)	7.97 (7.97)
	Cl		10.29 (10.29)		
Conductance ($ohm^{-1}cm^1 \cdot mol^{-1}$)		14	16	13	14
Absorption (nm) $\pi \rightarrow \pi^*$, $n \rightarrow \pi^*$, L→M		232, 280, 550	280, 300, 430	286, 515	276, 325
d-d transition				650	550, 680

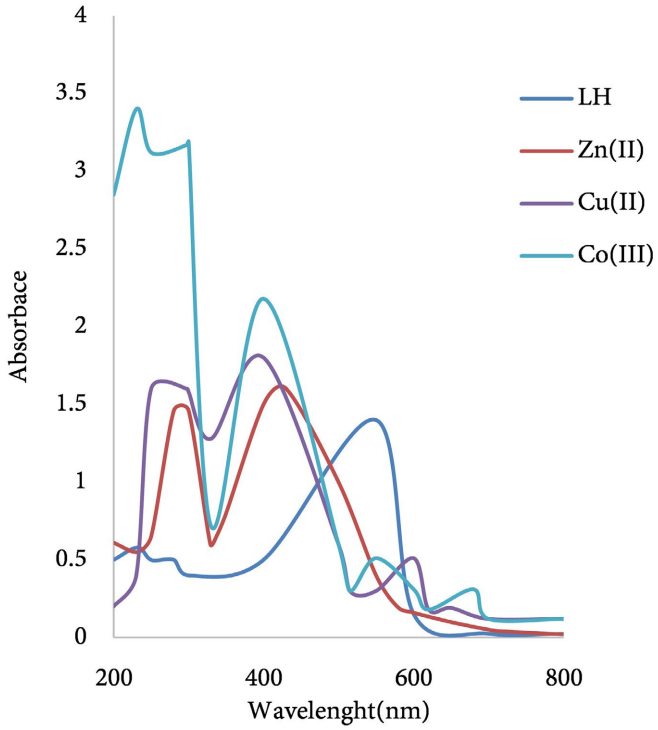

Figure 15. Electronic spectra of ligand LH and its metal complexes.

The LH ligand was found to exhibit two prominent bands at 232 nm associated with $\pi \rightarrow \pi$ transitions of the aromatic rings and at 280 nm as well as at 550 nm associated with $n \rightarrow \pi$ transitions (C=N) [24]. The magnetic moment of the Co (III) complex was found to be 0.06 BM, while the electronic spectrum of the Co (III) complex also displayed two broad absorption bands at 550 nm and 680 nm which may be assigned the $^1A_{1\,g} \rightarrow {}^1T_{2\,g}$ and $^1A_{1\,g} \rightarrow {}^1T_{1\,g}$ d-d transitions, respectively, which suggest low-spin diamagnetic octahedral geometry of the Co (III) complex [30] [31] [34]. The Cu (II) complex had a magnetic moment value of 1.76 B.M., which shows the presence of unpaired electrons, and the electronic spectra of the complex showed absorption bands at 298 nm assigned to intra-ligand charge transfer and that at 500 nm could be ascribed to ligand-to-metal charge transfer, while the weak band at 650 nm could be associated with d-d transition corresponding to $^2B_{1\,g} \rightarrow {}^2A_{1\,g}$, suggesting tetrahedral geometry around the Cu (II) ion [35]. The Zn (II) complex, with a magnetic moment of 0.05 B.M., was diamagnetic and the electronic spectrum shows only an intra-ligand transition at 280 - 300 nm, and absorption at 430 nm is associated with LTM charge transfer, and a tetrahedral geometry was proposed for this complex. Due to the complete d^{10} electronic configuration, a d-d transition band was not observed [10] [35].

3.3. Geometry Optimization

Quantum mechanical density functional theory calculations were carried out using the recently developed meta-generalized-gradient approximation (mGGA) composite method r2SCAN-3c [36] [37] with the ORCA program package (ORCA

6.0.1) to gain a better insight into the proposed molecular structures of the complexes, since their single crystals could not be isolated. The correct stereochemistry was assured through the exploitation and modification of the molecular coordinates to attain reasonable low-energy molecular geometries. The minimum steric energies, which were determined separately, resulted in global minimum energies of −967.7038, 3317.5468, 3715.3296, and 3.5765 kJ/mol for the ligand (LH) and its metal complexes—cobalt (III), zinc (II), and copper (II) complexes, respectively. The analytical and spectral studies suggested hexa-coordination for the cobalt (III) complexes and tetra-coordination for zinc (II) and copper (II) complexes, which were further optimized to obtain the most stable conformers (**Figures 16** and **Figures 17(a)-(c)**). The selected bond lengths and bond angles [28] [37] of the optimized complexes are presented in **Table 4**.

In the optimized structure of the cobalt (III) complex, Co(22)-N(12), Co(22)-N(18), N(34)-Co(22), N(40)-Co(22), Co(22)-O(16), and O(38)-Co(22) bond lengths are 2.0186 Å, 2.1086 Å, 1.9740 Å, 2.0233 Å, 1.8035 and 1.8316 Å, respectively, and the N(12)-N(13), N(33)-N(34) bond lengths of the ligand's azide group coordinating to Co (III) are 1.3686 Å and 1.3629 Å as opposed to the bond lengths of 1.3820 Å and 1.3592 Å for the C(17)-N(18), C(39)-N(40) azomethine pyridinyl nitrogen along with bond length values of 1.2261 Å, 1.2245 Å obtained for C(14)-O(16), C(36)-O(38) for the carbonyl moiety coordinating to Co (III). The corresponding bond angles N(12)-Co(22)-N(34), N(18)-Co(22)-N(40), O(16)-Co(22)-O(38), and O(38)-Co(22)-N(12) between the different functional donor groups of the ligand were found to be 90.4˚, 124.3˚, 103.4˚, and 170.7˚, respectively, which are very close to those reported by Mohamed *et al.* (2023) [38].

In the case of the copper (II) complex, the optimized structure gave Cu(43)-N(18), N(39)-Cu(43), Cu(43)-O(15), and O(37)-Cu(43) bond lengths to be 1.9442 Å, 1.9564 Å, 1.9153 Å, and 1.9235 Å respectively, while the ligand group donor sites C(17)-N(18), C (38)-N(39) azomethine pyridinyl nitrogen donor sites bond lengths were found to be 1.3408 Å each, as opposed to 1.2374 Å and 1.2363 Å for the O (15)-C (14) and C (35)-O (37) carbonyl oxygen donor sites. The associated bond angles N(18)-Cu(43)-N(39), N(39)-Cu-O (37), O(15)-Cu(43)-O(37) and O(37)-Cu(43)-N(18) were 111.0˚, 104.8˚, 120.8˚, and 110.4˚. In either case of Zn (II) and Cu (II) complexes, the variation in bond angles signifies a distorted tetrahedral environment around the metal (II) center [38].

In the optimized structure of the zinc (II) complex, the Zn(43)-N(18), N(39)-Zn(43), Zn(43)-O(15), and O(37)-Zn(43) bond lengths are respectively 1.8404 Å, 1.8786 Å, 1.8831 Å, and 1.9544 Å, while the C(17)-N(18), C(38)-N(39) azomethine pyridinyl nitrogen groups, along with O(15)-C(14) and C(35)-O(37) of the carbonyl groups of the ligand, are 1.2440 Å and 1.2516 Å respectively, in tetra-coordination to the Zn (II) center. The associated bond angles N(18)-Zn(43)-O(15), N(39)-Zn(43)-O(15), N(18)-Zn(43)-N(39), and O(37)-Zn(43)-O(15) were determined to be 102.3˚, 110.5˚, 112.7˚, and 128.4˚ respectively, which are in line with previously reported results in similar compounds [38]-[40].

Table 4. The calculated bond lengths and bond angles of metal (II/III) complexes.

Length (Å)						
Atom	Atom	LH ligand	Fe (II) complex	Co (III) complex	Zn (II) complex	Cu (II) complex
N17	C16	1.3566	1.3815	1.3820	1.3372	1.3408
N17	C18	1.3526	1.3644	1.4091	1.3675	1.3718
O14	C13	1.2291	1.2694	1.2261	1.2440	1.2374
O21	C8	1.2261	1.2175	1.2202	1.2184	1.2363
N11	C10	1.3861	1.4434	1.4587	1.4500	1.3411
N12	C13	1.3830	1.3724	1.3344	1.3656	1.3709
O7	C4	1.4052	1.3251	1.3261	1.3244	1.3604
O7	C8	1.3799	1.3276	1.3271	1.3201	1.3604
N1I	N12	1.3995	1.3714	1.3686	1.3851	1.3622
C8	C9	1.4681	1.4010	1.4926	1.4978	1.4176
C9	C10	1.3410	1.4051	1.4169	1.4192	1.4144
C13	C15	1.4771	1.5528	1.4926	1.4979	1.4894
C15	C16	1.3872	1.3877	1.4378	1.3871	1.3945
C18	C19	1.3861	1.4106	1.4250	1.4170	1.4711
C19	C20	1.3922	1.4308	1.4056	1.4217	1.4175
Angle (˚)						
Atom	Atom	Atom	LH ligand	Fe (II) complex	Co (III) complex	Zn (II) complex	Cu (II) complex
C5	N13	N14	115.9802	118.1234	120.3402	121.8126	117.4719
C16	N14	N13	123.9477	123.68506	124.6244	125.4414	124.0348
N14	C16	O18	118.5901	122.9612	119.6602	120..4461	118.9681
C17	C16	N14	120.1222	122.1311	124.8622	124.6482	123.6426
C17	C16	O18	121.8192	124.4526	122.8892	123. 2829	124.9684
N13	C5	O6	112.6980	114.9351	113.0986	115.6608	115.2862
C12	C7	O6	118.1211	119.3415	117.9232	121.1211	115.8921
C4	C5	N13	114.1713	116.7714	119.3713	115.1641	114.4793
C7	O6	C5	117.8211	114.6232	115.5292	116.5201	113.5428
C23	N22	C21	116.0625	115.8424	113.8432	114.4611	115.4621
C20	C21	N22	115.1711	113.0421	111.6318	114.5061	112.2743
C17	C23	N22	115.9201	110.1101	113.2111	114.6201	112.9701
C4	C3	O2	123.4602	119..5411	121.2612	122.3301	120.2302
C8	C3	O2	121.0288	121.6214	118.1222	120.1266	119.4422

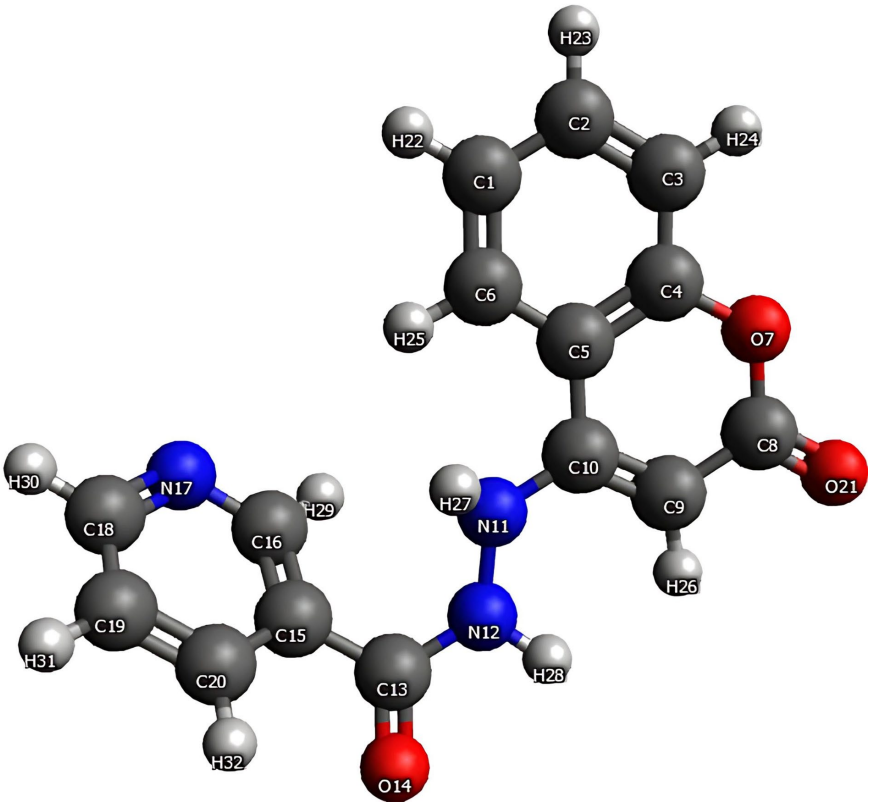

Figure 16. Optimized structure of the ligand.

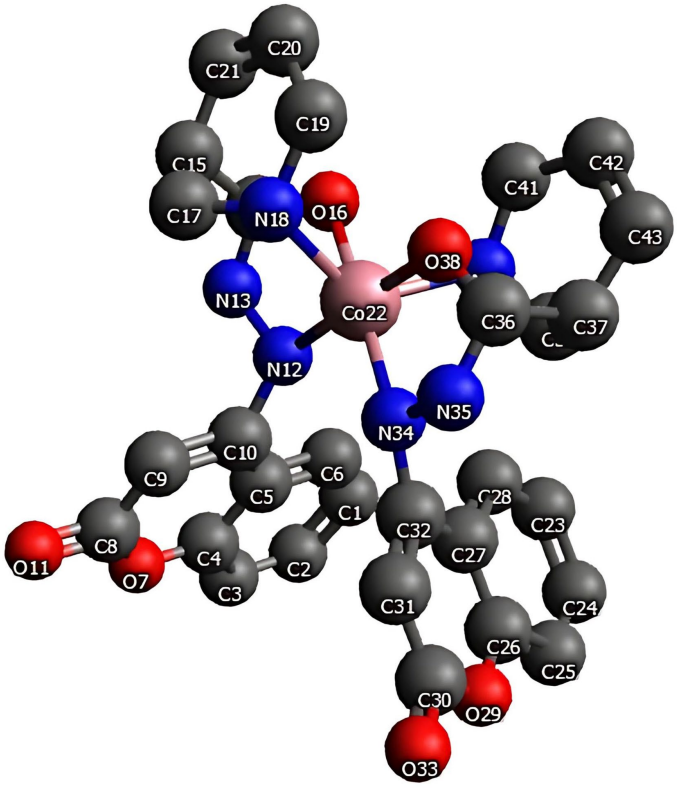

(a)

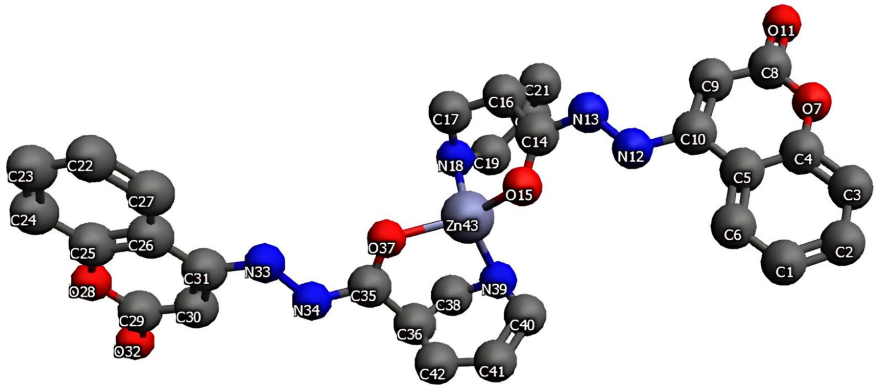

(b)

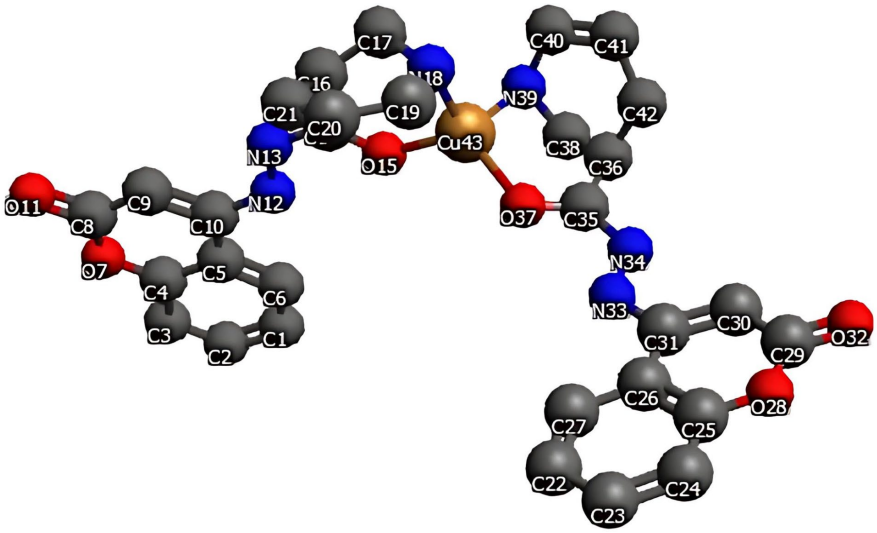

(c)

Figure 17. Molecular structures of: (a) Cobalt (III) complex, (b) Zinc (II) complex, and (c) Copper (II) complex.

4. Anti-Tuberculosis Activity

The hydrazone ligand LH and its metal (II)/metal (III) complexes were evaluated against *Mycobacterium tuberculosis* using streptomycin, pyrazinamide, and isoniazid as standard references. The results are presented in Table 5. The zinc (II) and copper (II) complexes have MIC 3.12 ± 0.34 μg/mL, which is the same as that of pyrazinamide and isoniazid, compared to the parent ligand (LH) with MIC value 6.25 ± 0.72 μg/mL, while the cobalt (III) complex with MIC value of 12.5 ± 1.20 μg/mL is higher than all of the standard drugs used, and the parent ligand (LH) is the least potent of all the synthesized compounds against the tested microorganisms.

Table 5. Anti-tubercular activity of ligand and its metal (II) complexes*.

Test sample	Sample concentration in MIC (μg/mL) ± SD
Ligand (LH)	6.25± 0.72

Continued

$Co(LH)_2(Ac)_2$	12.5 ± 1.20
$Zn(LH)_2$	3.12 ± 0.34
$Cu(LH)_2$	3.12 ± 0.34
Streptomycin	6.25± 0.72
Pyrazinamide	3.12± 0.34
Isoniazid	3.12± 0.34

*Values expressed are mean ± SD of three parallel measurements.

5. Conclusion

The compounds zinc (II), copper (II), and cobalt (III) complexes have been synthesized from a hydrazone ligand derived from nicotinic acid hydrazide and 4-hydroxycoumarin. The prepared compounds were characterized using FT-IR, thermal analysis, ^{1}H NMR spectroscopy, and investigated for anti-tuberculosis activities. The compounds were found to be hexa-coordinated for the cobalt (III) complex but tetra-coordinated for the copper (II) and zinc (II) complexes, in which the Schiff base ligand chelates to the metal centers in a tridentate mode through the azomethine nitrogen and the amide oxygen atoms. The anti-mycobacterial activities of the compounds showed zinc (II) and copper (II) complexes having identical activity to the reference drugs, pyrazinamide and isoniazid, while the cobalt (III) complex had the highest MIC value compared to the reference drugs and parent ligand. The anti-tubercular activity of ligand LH and its metal (II) complexes is quite promising as shown in the table, but its Cu (II) and Zn (II) complexes displayed a significant level of activity on the clinical isolates.

Acknowledgements

1) This work was supported (in part) by the Nanotechnology Platform of MEXT, Grant Number JPMXP09S20NR0016. This work was also supported by a Grant-in-Aid for Scientific Research (A) KAKENHI (20H00336). The authors are grateful to Professor Susan A. Bourne of Cape Town University in South Africa for the spectral analysis.

2) The authors are grateful to Professor Andrew D. Burrows of the Department of Chemistry, University of Bath, Bath Spa, United Kingdom, for assistance with spectroscopic measurements.

Conflicts of Interest

The authors declare no conflicts of interest regarding the publication of this paper.

References

[1] Sharma, P.C., Sharma, D., Sharma, A., Saini, N., Goyal, R., Ola, M., *et al.* (2020) Hydrazone Comprising Compounds as Promising Anti-Infective Agents: Chemistry and Structure-Property Relationship. *Materials Today Chemistry*, **18**, Article ID: 100349.

https://doi.org/10.1016/j.mtchem.2020.100349

[2] Walke, A.W. and Kathale, N.E. (2021) Synthesis and Characterization of Some Metal Complexes Prepared from Schiff Base Ligand Having Heterocyclic Unit. *Journal of Scientific Research*, **65**, 28-33. https://doi.org/10.37398/jsr.2021.650604

[3] Czyżewska, I., Mazur, L., Biernasiuk, A., Hordyjewska, A. and Popiołek, Ł. (2024) Synthesis, Structural Properties and Biological Activities of Novel Hydrazones of 2-, 3-, 4-Iodobenzoic Acid. *Molecules*, **29**, Article 3814. https://doi.org/10.3390/molecules29163814

[4] Ribeiro, N. and Correia, I. (2024) A Review of Hydrazide-Hydrazone Metal Complexes' Antitumor Potential. *Frontiers in Chemical Biology*, **3**, Article 1398873. https://doi.org/10.3389/fchbi.2024.1398873

[5] Tafere, D.A., Gebrezgiabher, M., Elemo, F., sani, T., Atisme, T.B., Ashebr, T.G., *et al.* (2025) Hydrazones, Hydrazones-Based Coinage Metal Complexes, and Their Biological Applications. *RSC Advances*, **15**, 6191-6207. https://doi.org/10.1039/d4ra07794f

[6] Kargar, H., Fallah-Mehrjardi, M., Ashfaq, M., Munawar, K.S. and Tahir, M.N. (2023) Cis-Dioxomolybdenum(VI) Complex Bearing Tridentate ONO Isonicotinoyl Hydrazone Schiff Base: Synthesis, Characterization, Crystal Structure, and Catalytic Activity Investigation for the Oxidation of Sulfides. *Journal of Molecular Structure*, **1294**, Article ID: 136458. https://doi.org/10.1016/j.molstruc.2023.136458

[7] Popiołek, Ł. (2021) Updated Information on Antimicrobial Activity of Hydrazide-Hydrazones. *International Journal of Molecular Sciences*, **22**, Article 9389. https://doi.org/10.3390/ijms22179389

[8] Elena, P., Diana-Carolina, L., Sergiu, S., Camelia, O., Virgil, P., Octavian, T.O., Flavian, S.R., Aurelian, G., Tudor, R. and Doina, D.(2017) Synthesis, Characterization, Antimicrobial and Antiproliferative Activity Evaluation of Cu(II), Co(II), Zn(II), Ni(II) and Pt(II) Complexes with Isoniazid-Derived Compound. *Molecules*, **22**, Article 650.

[9] Akramullazi, A., Sultana, S., Hossen, F., Asraf, A. and Kudrat-e-Zahan, (2024) Isonicotinohydrazide Derived Schiff Base-Transition Metal Complexes: Structure with Biological Activity. *International Journal of Chemistry Research*, **8**, 1-9. https://doi.org/10.22159/ijcr.2024v8i3.230

[10] Abouel-Enein, S.A., Emam, S.M. and Abdel-Satar, E.M. (2023) Bivalent Metal Chelates with Pentadentate Azo-Schiff Base Derived from Nicotinic Hydrazide: Preparation, Structural Elucidation, and Pharmacological Activity. C*hemistry and Biodiversity*, **20**, e202201223.

[11] Bansod, A., Bhaskar, R., Ladole, C., Salunkhe, N., Thakare, K. and Aswar, A. (2022) Synthesis, Characterization, Biological Activity and Solid-State Electrical Conductivity Study of Some Metal Complexes Involving Pyrazine-2-Carbohydrazone of 2-Hydroxyacetophenone. *Journal of Transition Metal Complexes*, **5**, 1-14. https://doi.org/10.32371/jtmc/246138

[12] Agili, F. (2024) Novel Hydrazide Hydrazone Derivatives as Antimicrobial Agents: Design, Synthesis, and Molecular Dynamics. *Processes*, **12**, Article 1055. https://doi.org/10.3390/pr12061055

[13] Knittl, E.T., Abou-Hussein, A.A. and Linert, W. (2017) Syntheses, Characterization, and Biological Activity of Novel Mono- and Binuclear Transition Metal Complexes with a Hydrazone Schiff Base Derived from a Coumarin Derivative and Oxalyldihydrazine. *Monatshefte für Chemie—Chemical Monthly*, **149**, 431-443. https://doi.org/10.1007/s00706-017-2075-9

[14] Yordanov, D., Deneva, V., Georgiev, A., Vassilev, N., Vala, M., Zhivkov, I., *et al.*

(2021) 4-OH Coumarin Based Rotary Switches: Tautomeric State and Effect of the Stator. *Dyes and Pigments*, **184**, Article ID: 108861. https://doi.org/10.1016/j.dyepig.2020.108861

[15] Kim, S.Y., Hong, H.C., Kim, J.H., Ryu, J.W., Choi, H.S., Chung, Y.T., *et al.* (2009) An Alternative Approach to Tuberculosis Management with Intravenous Streptomycin. *Infection and Chemotherapy*, **42**, 39-42. https://doi.org/10.3947/ic.2010.42.1.39

[16] Ashrafuzzaman, Uddin, E., Islam, R., Bitu, N.A., Hossain, S., Uddin, N., *et al.* (2020) Biological Applications of Isoniazid Derived Schiff Base Complexes: An Overview. *Asian Journal of Research in Biochemistry*, **6**, 17-31. https://doi.org/10.9734/ajrb/2020/v6i330118

[17] Toh-Boyo, G.M., Njong, R.N., Babette, E.M. and Nfor, E.N. (2021) Synthesis, Spectroscopic, Molecular Modeling and Anti-Fungal Studies of Some Divalent Metal Complexes of 4-Hydroxyacetophenone Isonicotinoyl Hydrazone. *Open Journal of Inorganic Chemistry*, **11**, 95-109. https://doi.org/10.4236/ojic.2021.113007

[18] Mikwa, C.C., Toh-Boyo, G.M., Njong, R.N., Ndoye, B.N., Ndamyabera, C.A., Katsuumi, N., *et al.* (2022) Bivalent Metal Complexes of a Novel Modified Nicotinic Acid Hydrazide Drug: Synthesis, Characterization, and Anti-Tubercular Studies. *European Journal of Chemistry*, **13**, 63-68. https://doi.org/10.5155/eurjchem.13.1.63-68.2183

[19] Kurbah, S.D. and Clovis, N.S. (2023) Coumarin-Hydrazone-Based Fluorescence Sensor for Al(III) Detection in Aqueous Solution: DFT Calculation and DNA Interaction Studies. *European Journal of Chemistry*, **14**, 330-336. https://doi.org/10.5155/eurjchem.14.3.330-336.2432

[20] Yadav, S. and Kumar, N. (2021) Synthesis and Evaluation of Novel 4-Hydroxycoumarin Derivatives as Potential Anti-Microbial Agents. *Oriental Journal of Chemistry*, **37**, 1132-1138. https://doi.org/10.13005/ojc/370517

[21] Khan, M.S., Agrawal, R., Ubaidullah, M., Hassan, M.I. and Tarannum, N. (2019) Design, Synthesis and Validation of Anti-Microbial Coumarin Derivatives: An Efficient Green Approach. *Heliyon*, **5**, e02615. https://doi.org/10.1016/j.heliyon.2019.e02615

[22] Verma, G.G., *et al.* (2022) Extraction of Coumarin from Ncinnamon and Examination of Its Antibacterial Activity. *Journal of Emerging Technologies and Innovative Research*, **9**, 288-297. https://www.jetir.org

[23] Todorov, L.T. and Kostova, I.P. (2024) Coumarin-Transition Metal Complexes with Biological Activity: Current Trends and Perspectives. *Frontiers in Chemistry*, **12**, Article 1342772. https://doi.org/10.3389/fchem.2024.1342772

[24] Todorov, L., Saso, L. and Kostova, I. (2023) Antioxidant Activity of Coumarins and Their Metal Complexes. *Pharmaceuticals*, **16**, Article 651. https://doi.org/10.3390/ph16050651

[25] Devi, J., Arora, T., Rani, G. and Rani, M. (2025) Hydrazone Ligands and Their Metal Chelates: A Confluence of Spectroscopic, Biological, and Computational Discoveries. *Research on Chemical Intermediates*. https://doi.org/10.1007/s11164-025-05724-z

[26] Yoda, J., *et al.* (2019) Review on 4-Hydroxycoumarin Chemistry: Synthesis, Acylation and Photochemical Properties. *World Journal of Organic Chemistry*, **7**, 19-30.

[27] Snyder, H.D. and Kucukkal, T.G. (2021) Computational Chemistry Activities with Avogadro and ORCA. *Journal of Chemical Education*, **98**, 1335-1341.

[28] Ariefin, M. and Alfanaar, R. (2023) Molecular Modelling Based on TD-DFT Applied to UV Spectra of Coumarin Derivatives. *Walisongo Journal of Chemistry*, **6**, 61-68. https://doi.org/10.21580/wjc.v6i1.15696

[29] Ahmed, A.H. and Mostafa, M.M. (2022) Physicochemical and Analytical Studies of Some Monomer and Polymer Complexes Derived from Selected Aroyl Hydrazone. *Open Journal of Inorganic Chemistry*, **12**, 1-17. https://doi.org/10.4236/ojic.2022.121001

[30] Abouzayed, F.I., Abouel-Enein, S.A. and Hammad, A.M. (2021) Synthesis of Some Novel Nanosized Chelates of Anchoring Bisazo Dye 5-[5-(4,6-Dioxo-2-Thioxo-Hexahydro-Pyrimidin-5-Ylazo)-Naphthalen-1-Ylazo]-2-Mercapto-1*h*-Pyrimidine-4,6-Dione and Their Applications as Antioxidant and Antitumor Agents. *ACS Omega*, **6**, 27737-27754. https://doi.org/10.1021/acsomega.1c02989

[31] Tolan, D.A., Kashar, T.I., Yoshizawa, K. and El-Nahas, A.M. (2021) Synthesis, Spectral Characterization, Density Functional Theory Studies, and Biological Screening of Some Transition Metal Complexes of a Novel Hydrazide-Hydrazone Ligand of Isonicotinic Acid. *Applied Organometallic Chemistry*, **35**, e6205. https://doi.org/10.1002/aoc.6205

[32] Nalini, R., Basavarajaiah, S.M., Nagesh, G.Y., Mohammad, J. and Ramakrishna Reddy, K. (2022) Synthesis, Characterization, DFT Analysis, Biological Evaluation, and Molecular Docking of Schiff Base Derived from Isatin-Isoniazid and Its Metal (II) Complexes. *Polycyclic Aromatic Compounds*, **43**, 7597-7614. https://doi.org/10.1080/10406638.2022.2138927

[33] Maghraoui, N., Aggoun, D., Bouzerafa, B., Bezzi, H., Ouennoughi, Y., López, D., *et al.* (2021) Synthesis, Characterization, Thermal Stability, Electrochemical Behavior, and Antioxidant Activity of New Oxovanadium(IV) and Iron(II) Tetradentate Schiff Base Complexes. *Arabian Journal of Chemistry*, **14**, Article ID: 103025. https://doi.org/10.1016/j.arabjc.2021.103025

[34] Kumar, L.V. and Nath, G.R. (2019) Synthesis, Characterization and Biological Studies of Cobalt(II), Nickel(II), Copper(II) and Zinc(II) Complexes of Vanillin-4-Methyl-4-Phenyl-3-Thiosemicarbazone. *Journal of Chemical Sciences*, **131**, Article No. 76. https://doi.org/10.1007/s12039-019-1658-x

[35] Ahmed, F., AbdAlqader, B., Haddad, R., Abed, R. and Saleh, M. (2022) Preparation and Diagnosis of Zn(II), Cd(II) and Hg(II) Complexes with Schiff Base Ligand Derived from Trimethoprim. *Egyptian Journal of Chemistry*, **6**, 359-366. https://doi.org/10.21608/ejchem.2022.119210.5362

[36] Alanís-Manzano, E.I., León-Pimentel, C.I., Maron, L., Ramírez-Solís, A. and Saint-Martin, H. (2024) Exploring the Dynamic Coordination Sphere of Lanthanide Aqua Ions: Insights from R^2SCAN-3c Composite-DFT Born-Oppenheimer Molecular Dynamics Studies. *ACS Omega*, **9**, 50978-50991. https://doi.org/10.1021/acsomega.4c04947

[37] Venkatesh, G., Vennila, P., Kaya, S., Ahmed, S.B., Sumathi, P., Siva, V., *et al.* (2024) Synthesis and Spectroscopic Characterization of Schiff Base Metal Complexes, Biological Activity, and Molecular Docking Studies. *ACS Omega*, **9**, 8123-8138. https://doi.org/10.1021/acsomega.3c08526

[38] Shehata, M., Shoukry, M. and Mabrouk, M. (2023) Metal Complexes of 1,4-Bis(2-Hydroxyethyl) Piperazine: Thermodynamic and Theoretical Approach. *Egyptian Journal of Chemistry*, **66**, 389-401. https://doi.org/10.21608/ejchem.2023.187495.7476

[39] Groneck, E.N., Peek, N., Lynch, W.E. and Padgett, C.W. (2025) Crystal Structures of Zinc(II) Coordination Complexes with Isoquinoline *n*-Oxide. *Acta Crystallographica Section E Crystallographic Communications*, **81**, 132-139.

https://doi.org/10.1107/s2056989025000180

[40] Enamullah, M., Anwar Hossain, M., Islam, M.K., Woschko, D. and Janiak, C. (2021) Pseudotetrahedral Copper(II)-Complexes with Enantiopure (*R* or *S*)-2-(((Aryl) Ethylimino)Ethyl)phenolate Schiff Base Ligands. *Dalton Transactions*, **50**, 9236-9249. https://doi.org/10.1039/d1dt01671g